KAERI/TR-2586/2003

A Comparison of Thermal Algorithms of Fuel Rod Performance Code Systems

2003. 11.

KOREA ATOMIC ENERGY RESEARCH INSTITUTE

제 출 문

한국원자력연구소장 귀하

본 보고서를 2003년도 "건식재가공 핵연료성능 평가기술 개발" 과제의 기술보고서로 제출합니다.

제목: 핵연료봉 성능평가용 전산체계의 온도계산 알고리듬 비교

2003. 11.

과제명 : 건식재가공 핵연료성능 평가기술개발

주저자 : 박창제

부저자 : 박주환, 강권호, 류호진, 문제선, 정인하, 이철용, 송기찬

ABSTRACT

The goal of the fuel rod performance is to identify the robustness of a fuel rod with cladding material. Computer simulation of the fuel rod performance becomes one of important parts to designed and evaluate new nuclear fuels and claddings. To construct a computing code system for the fuel rod performance, several algorithms of the existing fuel rod performance code systems are compared and are summarized as a preliminary work. Among several code systems, FRAPCON, and FEMAXI for LWR, ELESTRES for CANDU reactor, and LIFE for fast reactor are reviewed. Thermal algorithms of the above codes are investigated including methodologies and subroutines. This work will be utilized to construct a computing code system for dry process fuel rod performance.

TABLE OF CONTENTS

TABLE CONTENT

FIGURE CONTENT

I. INTRODUCTION

The purpose of the fuel rod performance analysis is simply stated as follows: for the given the geometry of the fuel element (i.e., the fuel radius, the cladding thickness, and the size of the fuel-cladding gap), the initial chemical composition and porosity of the fuel, and the power history during the irradiation should be predicted by function of time whether the integrity of cladding can be sustained its primary function. The thermal and mechanical behaviors of fuel rod during irradiation depend on a great number of individual phenomena and only a few of them are adequately understood theoretically. The computer simulations, which are called fuel rod performance codes, only attempt to follow the evolution of the important characteristics of the fuel and cladding as functions of irradiation time, beginning with the first application of power and temperature in failure by cladding rupture. The inputs of the code system consist in part simply of a list of physical, chemical, or mechanical properties or they may represent calculations of the rates of particular processes by subroutines nearly as large as the main fuel-modeling program. These material input functions can either be based entirely on theory or be derived form observations.[1]

There are many research activities to develop computer code systems for fuel rod performance since commercial nuclear reactor began. Among them, we choose several code systems to grasp the computational algorithm such as FRAPCON, FEMAXI, ELESTRES, and LIFE. Table I shows a simple comparison of characteristics of the above code systems. Figs. 1, 2, 3, and 4 show the schematic diagram of flowchart for FRAPCON, FEMAXI, ELESTRES, and LIFE, respectively. In this report, thermal and mechanical models are compared concentrating on treatment of models in each code system. Chapter II deals with thermal algorithm of FRAPCON-3 code system and in Chapter III, thermal algorithm of FEMAXI-V is provided. Thermal algorithms of CANDU and fast reactors are also compared in this report. Thermal algorithms of ELESTRES and LIFE are described

in Chapter IV and V, respectively. In Chapter VI, a brief summary the feasible thermal algorithm development of dry process fuel rod performance. A conclusion of this study is given in Chapter VII.

II. THERMAL ALGORITHM OF FRAPCON

The temperature distribution throughout the fuel and the cladding is calculated at each axial node. The models used in the fuel rod temperature calculations assume a cylindrical fuel pellet boundary conditions (coolant inlet temperature, coolant channel equivalent heated diameter, and time coolant mass flux) and the axial linear heat generation rate are used to calculate the coolant bulk temperature using a single channel coolant enthalpy rise model. A film temperature rise is then calculated from the coolant to the surface of the fuel rod through any crud layer which may exist. The cladding inside surface temperature is calculated by the temperature rise across the zirconium oxide and the cladding using Fourier's law. The temperature rise to the fuel surface is determined from an annular gap conductance model, thereby establishing the fuel surface temperature. Finally, the temperature distribution in the fuel is calculated, accounting for fuel cracking effects using the fuel surface temperature and assumed symmetry at the centerline as boundary conditions.[2] A simplified flowchart of the temperature distribution solution is shown Fig. 5.

The models used in the temperature calculations involve a number of assumptions and limitations as follows:

(a) Heat conduction in the axial direction is considered negligible relative to radial heat conduction and is ignored.

(b) Heat conduction in the azimuthal direction is ignored (axisymmetric analysis).

(c) Constant boundary conditions are maintained during each time step.

(d) Steady-state heat flow is assumed.

(e) The fuel rod is a right circular cylinder surrounded by water coolant.

II.A Coolant Conditions

FRAPCON-3 calculates bulk coolant temperatures assuming a single, closed coolant channel according to

$$T_b(z) = T_{in} + \int_0^z \left\{ \frac{4q''(z)}{C_p G D_e} \right\} dz \,, \tag{1}$$

where

$T_b(z)$ = bulk coolant temperature at elevation z on the rod axis (K),

T_{in} = inlet coolant temperature (K),

$q''(z)$ = rod surface heat flux at elevation z on the rod axis (W/m^2),

C_p = heat capacity of the coolant (J/kg-K),

G = coolant mass flux (kg/s-m^2),

D_e = coolant channel heated diameter (m).

Coolant heat capacity is calculated using the following relationships:

$$\begin{aligned} C_p &= 2.4\times10^5 \ J/kg\cdot K, \quad T_b(z) < 544K \\ &= 2.4\times10^5[1+2.9\times10^{-3}\{1.8T_b(z)-1031\}, \quad 544K \le T_b(z) < 588K \\ &= 2.4\times10^5[1+2.9\times10^{-3}\{1.8T_b(z)-979.4\}, \quad T_b(z) \ge 588K \end{aligned} \tag{2}$$

Coolant channel heated diameter is calculated from rod pitch and diameter using the following relationship:

$$D_e = \frac{4.0\left\{(P_{pit})^2 - \pi(D_0)^2/4\right\}}{\pi D_0}, \tag{3}$$

where

P_{pit} = rod-to-rod pitch (m),

D_0 = outside cladding diameter (m).

II.B Fuel Rod Surface Temperature

The cladding surface temperature at axial elevation z is taken as the minimum value of

$$T_w(z) = T_b(z) + \Delta T_f(z) + \Delta T_{cr}(z) + \Delta T_{ox}(z), \quad (4)$$

$$T_w(z) = T_{sat} + \Delta T_{JL} + \Delta T_{ox}(z), \quad (5)$$

where

$T_w(z)$ = rod surface temperature at elevation z on the rod axis (K),

$\Delta T_f(z)$ = forced convection film temperature drop at elevation z on the rod axis (K),

$\Delta T_{cr}(z)$ = crud temperature drop at elevation z on the rod axis (K),

$\Delta T_{ox}(z)$ = oxide layer temperature drop at elevation z (K),

T_{sat} = coolant saturation temperature (K),

ΔT_{JL} = nucleate boiling temperature drop at elevation z on the rod axis (K) is determined by the Jens-Lottes (JL) correlation.

The choice of the minimum value is a simple means of deciding whether heat is transferred from the cladding surface to the coolant by forced convection or nucleate boiling. It also provides a smooth numerical transition form forced convection to nucleate boiling, thereby avoiding convergence problems. For forced-convection heat transfer, the temperature drop across the coolant film layer at the rod surface is based on

$$\Delta T_f(z) = q''(z)/h_f, \quad (6)$$

where h_f is the Dittus-Boelter film conductance given by

$$h_f = (0.023k/D_e)\,\mathrm{Re}^{0.8}\,\mathrm{Pr}^{0.4}, \quad (7)$$

where

h_f = conductance (W/m^2-K),

k = conductivity of the water (W/m-K),

D_e = coolant channel heated diameter (m),

Re = Reynolds number ($= \rho v A/\mu$),

ρ = density of coolant,

v = speed of coolant,

A = area of coolant flow,

μ = viscosity of coolant,

Pr = Prandtl number ($= C_p \mu / k$).

The temperature drop across the crud is given by

$$\Delta T_{cr}(z) = q''(z)\frac{\delta_{cr}}{k_{cr}}, \tag{8}$$

where

δ_{cr} = crud thickness (m),

k_{cr} = crud thermal conductivity, 0.8648(W/m-K).

For nucleate boiling heat transfer, the temperature drop across the coolant film layer at the rod surface is based on the Jens-Lottes formulation

$$\Delta T_{JL}(z) = 60\left\{q''(z)/10^6\right\}^{0.25} / e^{(p/6.2\times10^6)}, \tag{9}$$

where P is the system bulk coolant pressure (Pa).

It is assumed that the crud does not any resistance to heat flow during nucleate boiling, therefore, no temperature drop due to crud is calculated. The coolant is assumed to boil through the crud blanket. The temperature drop across the zirconium oxide layer at elevation z on the rod axis is determined by

$$\Delta T_{ox}(z) = q''(z)\frac{\delta_{ox}(z)}{k_{ox}}, \tag{10}$$

where

$\Delta T_{ox}(z)$ = oxide temperature drop at elevation z on the rod axis (K),

$\delta_{ox}(z)$ = oxide thickness at elevation z on the rod axis (m),

k_{ox} = oxide thermal (W/m-K).

II.C Cladding Temperature Drop

The cladding temperature drop for each axial location is calculated according to the following expression for steady-state heat transfer through a cylinder with uniform conductivity:

$$\Delta T_c = q''(z) r_o \ln(r_o / r_i) / k_c, \tag{11}$$

where

ΔT_c = cladding temperature drop (K),

r_o = cladding outside radius (m),

r_i = cladding inner radius (m),

k_c = temperature and mechanical dependent thermal conductivity of the cladding (W/m-K).

II.D Fuel-Cladding Gap Temperature Drop

The fuel cladding gap temperature drop is calculated using the fuel rod surface heat flux at elevation z and the fuel-cladding gap conductance. The fuel-cladding gap conductance is the sum of three components: the conductance due to radiation, the conduction through the gas, and the conduction through regions of solid-solid contact. The equations and models for each of these components are presented in the following sections.

$$\Delta T_{gap} = q''(z)/h, \tag{12}$$

where

$h = h_r + h_{gas} + h_{solid}$,

$q''(z)$ = rod surface heat flux at elevation z on the axis (W/m^2),

h_r = conductance due to radiation (W/m^2-K),

h_{gas} = conductance of the gas gap (W/m^2-K),

h_{solid} = conductance due to fuel-cladding contact (W/m^2-K).

The conductance due to radiation, h_r (W/m^2-K), is defined using the net surface heat flux (S.H.F) which is derived by Kreith and others:

$$\begin{aligned} S.H.F &= h_r(T_{fs} - T_{ci}) = \sigma F(T_{fs}^4 - T_{ci}^4), \\ h_r &= \sigma F(T_{fs}^2 + T_{ci}^2)(T_{fs} + T_{ci}), \end{aligned} \tag{13}$$

where

$F = 1/\{1/e_f + (r_{fs}/r_{ci})(1-1/e_c)\}$,

σ = Stefan-Boltzmann constant, 5.6697×10^{-8} (W/m^2-K^4),

e_f = fuel emmissivity,

e_c = cladding emissivity,

T_{fs} = fuel surface temperature (K),

T_{ci} = cladding inner surface temperature (K),

r_{fs} = fuel outer surface radius (m),

r_{ci} = cladding inner surface radius (K).

The form of the conductance due to net radiant heat transfer of heat transfer through the gas in the fuel-cladding gap, h_{gas} (W/m^2-K), is that universally applied to small annular graps:

$$h_{gas} = k_{gas} / \Delta x, \tag{14}$$

$$\Delta x = d_{eff} + 1.8(g_f + g_c) - b + d, \tag{15}$$

where

k_{gas} = gas thermal conductivity (W/m-K),

Δx = total effective gap width (m),

d = value from FRACAS for open fuel-cladding gap size (m),

d_{eff} = exp(-0.00125P) (R_f+R_c) for closed fuel-cladding gaps (m),

= (R_f+R_c) for open fuel-cladding gaps (m),

P = fuel-cladding interfacial pressure (kg/cm^2),

$R_f + R_c$ = cladding plus fuel surface roughness and cladding surface roughness (m),

$g_f + g_c$ = temperature jump distances at fuel and cladding surfaces, respectively (m),

b = 1.397×10^{-6} (m).

The quantity ($g_f + g_c$) is calculated from the GAPCON-2 model and is

$$(g_f + g_c) = A\left(\frac{k_{gas}\sqrt{T_{gas}}}{P_{gas}}\right)\left(\frac{1}{\sum a_i f_i / \sqrt{M_i}}\right), \tag{16}$$

where

A = 0.7816,

k_{gas} = gas conductivity (W/m-K),

P_{gas} = gas pressure (Pa),

T_{gas} = average gas temperature (K),

a_i = accommodation coefficient of i-th gas component,

M_i = gram-molecular weight of i-th gas component (k-moles),

f_i = mole fraction of i-th gas component.

The contact conductance model is a modification of the Mikic-Todreas model that preservers the roughness, conductivity, and pressure dependencies while providing a best-estimate for the range of contact conductances measured by Garnier and Begej. The FRACAS-I model uses expressions for h_{solid} that depend on both the fuel-cladding interfacial pressure and the microscopic roughness, R, as follows

$$\begin{aligned} h_{solid} &= \frac{5.0 K_m P_{rel} R_{mult}}{R E}, \quad P_{rel} > 0.003, \\ &= \frac{0.015 K_m}{R E}, \quad 9\times10^{-6} < P_{rel} < 0.003, , \\ &= \frac{5.0 K_m P_{rel}^{0.5}}{R E}, \quad P_{rel} < 9\times10^{-6}, \end{aligned} \tag{17}$$

where

P_{rel} = ratio of interfacial pressure to cladding Meyer hardness (approximately 680 MPa),

K_m = mean conductivity (W/m-K),

$= 2K_f K_c /(K_f + K_c)$,

$R = \sqrt{R_f^2 + R_c^2}\ (m)$,

$R_{mult} = 333.3 P_{rel}, \quad P_{rel} < 0.0087,$

$= 2.9, \quad P_{rel} > 0.0087,$

K_c = cladding thermal conductivity (W/m-K),

K_f = fuel thermal conductivity (W/m-K),

$E = \exp[5.738 - 0.528\ln(R_2)]$,

R_2 = roughness of the rougher surface.

II.E Fuel Pellet Heat Conduction Model

The steady-state integral form of the heat conduction equation is solved to determine temperature distribution of fuel pellet.

$$\iint_s k(T,x)\vec{\nabla}T(x)\cdot\vec{n}\,ds = \iiint_V S(x)dV\,, \tag{18}$$

where

k = thermal conductivity (W/m-K),

s = surface of the control volume (m^2),

$\vec{n}$ = the surface normal unit vector,

S = internal heat source (W/m^3),

T = temperature (K),

V = control volume (m^3),

x = the space coordinates (m).

The heat conduction model of fuel pellet is based on the finite difference approach used in RELAP5 and FRAPTRAN. Variable mesh spacing and the spatial dependence of the internal heat source is allowed. The following assumptions are made to develop: fixed geometry, symmetrical geometry, negligible heat conduction in the axial direction, negligible heat conduction in the azimuthal direction, steady-state, mesh point averaged thermal conductivity.

Two boundary conditions are needed to calculate the temperature profile in the fuel. The boundary conditions are the symmetry condition ($\partial T / \partial x|_{x=0} = 0$), at the center on the fuel pellet and a prescribed temperature at the surface of the fuel.

The left term of Eq. (18) is approximated by

$$\iint_s k(T,x)\vec{\nabla}T(x)\cdot\vec{n}\,ds \approx (T_{m-1}-T_m)k_{lm}\delta^s_{lm} + (T_{m+1}-T_m)k_{rm}\delta^s_{rm}, \tag{19}$$

where

$$\delta^s_{lm} = \frac{2\pi}{\delta_{lm}}(x_m - \frac{\delta_{lm}}{2}), \quad \delta^s_{rm} = \frac{2\pi}{\delta_{rm}}(x_m + \frac{\delta_{rm}}{2}). \tag{20}$$

The right term of Eq. (18) is also approximated as

$$\iiint_V S(x)dV \approx S_{lm}\delta^v_{lm} + S_{rm}\delta^v_{rm}, \tag{21}$$

where

$$\delta^v_{lm} = \frac{2\pi\,\delta_{lm}}{2}(x_m - \frac{\delta_{lm}}{4}), \quad \delta^s_{rm} = \frac{2\pi\,\delta_{rm}}{2}(x_m + \frac{\delta_{rm}}{4}). \tag{22}$$

Typical mesh points and notations are given in Fig. 6. Combining Eqs. (19) and (21), the basic finite difference equation for the m-th point is derived as follows:

$$a_m T_{m-1} + b_m T_m + c_m T_{m+1} = d_m, \tag{23}$$

where

$$a_m = -(k_{lm}\delta^s_{lm}), \quad c_m = -(k_{rm}\delta^s_{rm}), \quad b_m = -a_m - c_m, \; d_m = S_{lm}\delta^v_{lm} + S_{rm}\delta^v_{rm}. \tag{24}$$

Eq. (23) is solved by Gaussian elimination without additional matrix iterations.

The fuel thermal conductivity in FRAPCON-3 is based on the expression developed by Lucuta et al. The conductivity for irradiated urania is given by

$$k = k_0 \times FD \times FP \times FM \times FR, \tag{25}$$

where

k_0 = conductivity of unirradiated urania (W/m-K),

FD = The factor by the effect of the dissolved fission products,

FP = The factor by the effect of the precipitated fission products,

FM = The factor by the effect of porosity,

FR = The factor by the effect of in-reactor.

This expression includes the term developed by Harding and Martin for the conductivity (k_0) of unirradiated, fully dense urania, modified for urania-gadolinia or urania-plutonia:

$$k_0 = \frac{CR}{0.0375 + 2.165\times10^{-4}T + BG \times GAD} + \left(\frac{4.715\times10^{9}}{T^2}\right)\exp(-16361/T), \tag{26}$$

where

T = temperature (K),

GAD = gadolinia content, wt%,

BG = gadolinia degradation, = 0.0150 m-K/W per gadolinia weight %,

CR = 1.0 for urania or urania-gadolinia,

= ratio of mixed-oxide specific heat to urania specific heat for urania-plutonia.

The effect of burnup is to build dissolved and precipitated fission products into the matrix (FD and FP).

$$FD = \left(\frac{1.09}{B^{3.265}} + \frac{0.0643}{\sqrt{B}}\sqrt{T}\right)\arctan\left(\frac{1}{\frac{1.09}{B^{3.265}} + \frac{0.0643}{\sqrt{B}}\sqrt{T}}\right), \tag{27a}$$

$$FP = 1 + \left(\frac{0.019B}{3 - 0.019B}\right)\left(\frac{1}{1+\exp\left(-\frac{T-1200}{100}\right)}\right). \tag{27b}$$

where

B = burnup in atom % (1 atom%=9.383 GWd/MTU at 200 MeV/fission).

The effect of porosity is accounted for by the well known Maxwell factor, FM, given by

$$FM = \frac{1-p}{1+(s-1)p}, \tag{28}$$

where

p = porosity fraction (as-fabricated plus swelling),

s = shape factor (assumed = 1.5 for spherical pores).

The radiation effect (applied at all times) in-reactor is given by the factor FR:

$$FR = 1 - \frac{0.2}{1+\exp\left(\frac{T-900}{80}\right)}. \tag{29}$$

III. THERMAL ALGORITHMS OF FEMAXI

Analytical scope of FEMAXI-V covers normal operation conditions and transient conditions as well such as load-following and rapid power increase, and also boiling transition of BWR fuels. However, it does not cover such accident. Table II shows the phenomena analyzed by FEMAXI-V.

III.A Heat Transfer to Coolant and Thermal-Hydraulics Model

In the thermal analysis part, temperature distribution of a fuel rod is calculated with the boundary conditions determined by coolant temperatures and pressure. The basic assumption and calculation procedure are as follows:

a) Temperature and states of the coolant of all axial segments depend on enthalpy distribution of the coolant in a previous time step, and are determined by temperature, pressure and flow velocity at the inlet and surface heat flux from each segment in the current time step. The thermal-hydraulics model of FEMAXI-V can be applied not only to steady states, but also to transient changes such as increase/decrease in power and load-following condition under normal operation and also in the rapid change of coolant flow rate.
b) Enthalpy of each axial segment is calculated, on the basis of the enthalpy distribution at the end of the former time step, with the enthalpy of the coolant at the inlet as the initial value, using the increase in the enthalpy obtained from flow velocity and the amount of heat generation form each segment. Distribution of the coolant temperature in the axial direction is determined by thus-obtained distribution of the coolant enthalpy.
c) The heat transfer coefficient in each boiling or coolant mode is determined. Surface temperature of the cladding is then calculated with coolant temperature as a starting point.
d) Temperature distribution from the cladding surface to the pellet center is calculated in a radial one-dimensional system, using the results obtained in c) step as a boundary condition.
e) Heat transfer in the axial direction of a fuel rod is not taken into consideration, assuming that heat transfer in the axial direction due to the power distribution in the axial direction is suppressed by such thermal resistance as dishes and gap at the edge surface of pellet.

This thermal-hydraulics model includes coolant enthalpy increase model, determination of cladding surface heat transfer coefficient, and transition of coolant condition. In the coolant enthalpy increase model, mass flux and pressure during each time step are assumed to be constant and time step is determined by flow velocity at each axial segment. To determine cladding surface heat transfer coefficient, FEMAXI classified boiling of coolant into saturation boiling and surface boiling (sub-

cool boiling) depending on the liquid temperature, into in-tube boiling and pool boiling depending on the presence of flow, and into nucleate boiling, transition boiling and film boiling depending on the mode of the phenomenon. Different correlations of heat transfer coefficient are supposed depending on the boiling modes. The detail descriptions and equations are given in ref. 3.

III.B Determination of Cladding Surface Temperature

Like FRAPCON-3, the FEMAXI uses the finite difference equation of thermal conduction inside a fuel rod.

$$\Phi_N = A\,T_N + B, \tag{30}$$

where

Φ_N = cladding surface heat flux (W/m^2),

T_N = cladding surface heat flux (K),

N = cladding surface mesh number,

A, B = coefficients determined by the finite difference equation of thermal conduction.

Surface temperature T_N can be obtained from the heat transfer coefficient of a cladding surface determined using Eq. (30). That is, when coolant temperature is designated as T_B, heat flux at cladding surface can be given as

$$\Phi_N = h_w(T_N - T_B), \tag{31}$$

where

h_w = heat transfer coefficient of coolant (W/m^2-K).

Surface temperature T_N is derived using Eqs. (30) and (31) as

$$T_N = (h_w T_B + B)/(h_w - A). \tag{32}$$

III.C Determination of Cladding Surface Temperature

Unlike FRAPCON, the FEMAXI-V treats the temporal derivation of thermal conduction equation with finite difference approach. Volume-integrated thermal conduction equation is given as

$$\iiint_V \frac{\partial}{\partial t} C_v(T,x)T(x,t)dV = \iint_s k(T,x)\vec{\nabla}T(x)\cdot\vec{n}\,ds + \iiint_V S(x)dV\,, \tag{33}$$

where

C_v = volume specific heat (J/m^3),

t = time (s).

The first term is approximated as

$$\iiint_V \frac{\partial}{\partial t} C_v(T,x)T(x,t)dV = \iiint_V C_v(T,x)\frac{\partial T}{\partial t}(x,t)dV$$
$$\approx \frac{T_m^{n+1} - T_m^n}{\delta_{lm}}\left[C_{v,lm}\frac{\delta_{lm}}{2}\left(x_m - \frac{\delta_{lm}}{4}\right) + C_{v,rm}\frac{\delta_{rm}}{2}\left(x_m + \frac{\delta_{rm}}{4}\right)\right], \tag{34}$$

where T_m^n is the temperature at coordinate x_m and time t_n.

The right terms are similarly approximated way done in FRAPCON-3 and the time step is approximated using the Crank-Nicholson method. After some numerical manipulations, the final form of Eq. (33) is arranged as

$$a_m T_{m-1}^{n+1} + b_m T_m^{n+1} + c_m T_{m+1}^{n+1} = d_m^n, \tag{35}$$

where

$$\begin{aligned} &a_m = -(k_{lm}\delta_{lm}^s \Delta t)/2, \quad c_m = -(k_{rm}\delta_{rm}^s \Delta t)/2, \\ &b_m = D_m - a_m - c_m, \ D_m = C_{v,lm}\delta_{lm}^v + C_{v,rm}\delta_{rm}^v, \\ &d_m = -a_m T_{m-1}^n + (D_m + a_m + c_m)T_m^n - c_n T_{m+1}^n \\ &\quad + \Delta t\{(S_{lm}^n + S_{lm}^{n+1})\delta_{lm}^v + (S_{rm}^n + S_{rm}^{n+1})\delta_{rm}^v\}/2 \end{aligned} \tag{36}$$

Eq. (35) is also solved easily by the Gauss elimination method.

For the gap and the cladding regions, a simple finite difference approaches are used and the unknown variables are obtained from forward elimination and backward substitution of the Gaussian elimination method.

III.D Pellet Thermal Conductivity

In FEMAXI-V, 12 thermal conductivity models can be chosen including MATPRO model and Lucuta's model. It is known that the thermal conductivity is affected by porosity and density. The following equation holds between porosity p and theoretical density ratio D.

$$p(I) = 1.0 - D(I), \tag{37}$$

where

I = pellet ring element number.

$D(I)$ is defined as

$$D(I) = D_i - 3\Delta L / r, \tag{38}$$

where

D_i = initial theoretical density ratio,

ΔL = radial displacement due to volume change generated by irradiation,

r = pellet radius.

In FEMAXI-V, it is possible to specify $D(I)$ using net radial thickness change of ring element I by densification, swelling, and hot-press.

IV. THERMAL ALGORITHM OF ELESTRES

ELSTRES is a computer program designed to predict the behavior of CANDU fuel under normal operating conditions. It takes into account the fuel geometry, material properties and the operating conditions, and predicts the percentage fission gas release, internal gas pressure, radial temperature distribution, and the percentage elastic and plastic sheath strains in a fuel element. It can be used to generate the initial conditions for analysis using ELOCA - a one dimensional code for simulation of fuel behavior under transient conditions.

IV.A Temperature Distribution of Pellet

Computing the temperature distribution in the fuel pellet, given the surface temperature, is performed somewhat analytical approaches in ELESTRES. And finite difference method is used to determine the one dimensional temperature distribution.

The energy equation for a cylindrical pellet with internal heat generation is:

$$\frac{d}{dr}\left(kr\frac{dT}{dr} \right) + h_r r = 0, \tag{39}$$

where

k = thermal conductivity,

r = radial coordinate,

T = temperature,

h_r = heat generation rate per unit volume,

$$h_r = h_0\left\{ I_0(\kappa r) + \frac{I_1(\kappa b)}{K_1(\kappa b)} K_0(\kappa r) + \beta \exp(\lambda (r-a)) \right\}, \tag{40}$$

I_i = ith order modified Bessel function of first kind,

K_i = ith order modified Bessel function of second kind,

κ = neutron inverse diffusion length,

b = radius of central hole,

a = radius of pellet,

β = empirical constant in the flux depression term,

λ = empirical constant in the flux depression term,

h_0 = heat generation rate per unit volume at pellet centerline,

$$h_0 = \frac{P}{\pi a^2 H}, \tag{41}$$

P = linear power output of fuel element (kW/m),

H = average heat generation rate in the pellet (dimensionless) relative to the heat generation rate at centerline.

Boundary conditions:

(a) $\left.\frac{dT}{dr}\right|_{r=b} = 0$; no heat transfer through the inner surface

(b) $T(r=a) = TS$

Integrating Eq. (39) from b to a radius inside the pellet, and using boundary condition (a):

$$kr\left.\frac{dT}{dr}\right|_{b}^{r} + \int_{b}^{r} h_r r\, dr = 0, \tag{42}$$

This equation can now be written in finite difference form with the ith temperature node at the inner surface of annulus i.

To obtain more accuracy, a parabolic temperature distribution is assumed,

$$T = A - Br^2, \tag{43}$$

The corresponding gradient is

$$\frac{dT}{dr} = -2Br. \tag{44}$$

To get the coefficient B, T_i and T_{i+1} are used such as

$$\begin{aligned} T_i &= A - Br_i^2, \\ T_{i+1} &= A - Br_{i+1}^2, \end{aligned} \tag{45}$$

and solving for B

$$B = -\frac{T_{i+1} - T_i}{r_{i+1}^2 - r_i^2}. \tag{46}$$

Therefore, Eq. (44) is rewritten as

$$\frac{dT}{dr} = 2\frac{T_{i+1} - T_i}{r_{i+1}^2 - r_i^2} r = 2\frac{T_{i+1} - T_i}{(r_{i+1} - r_i)(r_{i+1} + r_i)} r\,, \tag{47}$$

and

$$\left.\frac{dT}{dr}\right|_{r=r_{i+1}} = \frac{1}{\Delta r}(T_{i+1} - T_i)\frac{2r_{i+1}}{(r_{i+1} + r_i)}. \tag{48}$$

where $\Delta r = r_{i+1} - r_i$.

Thus, Eq. (42) becomes in the finite difference form:

$$k_{i+1} r_{i+1} \frac{T_{i+1} - T_i}{\Delta r} \frac{2 r_{i+1}}{(r_{i+1} + r_i)} + \int_b^{r_{i+1}} h_r \, r \, dr = 0 , \tag{49}$$

where $k_{i+1} = k(T_{i+1})$.

Solving for T_i with integration, we obtain

$$\begin{aligned} T_i = T_{i+1} + \frac{r_{i+1} + r_r}{2 r_{i+1}} \frac{\Delta r}{k_{i+1} r_{i+1}} \times h_0 [\frac{1}{\kappa} \{ r_{i+1} I_1(\kappa r_{i+1}) - B I_1(\kappa b) \\ - \frac{I_1(\kappa b)}{K_1(\kappa b)} (r_{i+1} K_1(\kappa r_{i+1}) - b K_1(\kappa b)) \} + \frac{\beta}{\lambda^2} \exp(-\lambda a) \{ (\lambda r_{i+1} - 1) \exp(\lambda r_{i+1}) + 1 \}] \end{aligned} \tag{50}$$

and in the case of no central hole (b=0),

$$T_i = T_{i+1} + \frac{r_{i+1} + r_r}{2 r_{i+1}} \frac{\Delta r}{k_{i+1} r_{i+1}} \times h_0 [\frac{r_{i+1} I_1(\kappa r_{i+1})}{\kappa} + \frac{\beta}{\lambda^2} \exp(-\lambda a) \{ (\lambda r_{i+1} - 1) \exp(\lambda r_{i+1}) + 1 \}] . \tag{51}$$

In ELESTRES, Eq. (51) is used regardless of the presence of central hole.

IV.B Calculation of Parameters

As irradiation proceeds, the original fissile atoms are depleted, fission products build up, and new fissile atoms are formed. Since these processes are dependent on the neutron spectrum and local neutron flux, the local fission rate within the fuel pellet will vary with burnup. In practice, the build up of plutonium atoms near the fuel surface has the greatest effect, leading to higher fission rates at the surface and reduce average fuel temperatures as burnup proceeds. To approximate these effects, the ratio of the local fission rate (h_r) at radius r to the fission rate at the fuel center (h_0) is assumed as

$$h_r = h_0 \{ I_0(\kappa r) + \beta \exp(\lambda (r - a)) \} , \tag{52}$$

where κ, β and λ are constants that vary with burnup.

The HAMMER physics code is used to obtain the parameters κ, β and λ as a function of burnup. The values at each history point are obtained by interpolation routine from the data stored.

V. THERMAL ALGORITHM OF LIFE

LIFE-I is designed to predict the in-pile behavior of cylindrical fast-reactor fuel elements. Assuming axial symmetry, the generalized plane-strain analysis combines models for fuel restructuring, migration of fuel constituents, fuel swelling due to the accumulation of fission products, fission-gas release, hot pressing of the fuel, and cladding swelling due to void nucleation and growth.

V.A Coolant Temperature of Axial Node

Determine coolant temperature at the middle of each axial section $T_{Na}(n)$:

$$\int_{T_{in}}^{T_{Na}(n)} C_p dT = \frac{\sum_{i=1}^{n} QSF(i) - QSF(n)/2}{\sum_{i=1}^{NF} QSF(i)} \int_{T_{in}}^{T_{out}} C_p dT, \tag{53}$$

where

n = axial section number,

T_{in}= inlet coolant temperature for the element,

T_{out}= outlet coolant temperature for the element,

QSF(i) = axial power distribution factors,

NF= total number of axial fuel sections specified,

C_p= specified heat of the coolant.

Eq. (53) is solved numerically by Newton-Raphson method with Cp assumed to be a quadratic function of temperature such as

$$C_p = C_0 + C_1 T + C_2 T^2, \tag{54}$$

where

$C_0 = 0.3457,$

$C_1 = -0.792 \times 10^{-4},$

$C_2 = 3.41178 \times 10^{-8}.$

Newton-Raphson Method:

$$f(x) = 0 \;\rightarrow\; x_{i+1} = x_i - f(x_i)/f'(x_i) \tag{55}$$

Rewriting Eq. (53)

$$\int_{T_{in}}^{T_{in}+X} C_p dT = C, \tag{56}$$

$$\frac{B_2}{3} X^3 + \frac{B_1}{2} X^2 + B_0 X - C = 0, \tag{57}$$

where

$$C = (\sum_{i=1}^{n} QSF(i) - QSF(n)/2) / \sum_{i=1}^{NF} QSF(i) \times \int_{T_{in}}^{T_{out}} C_p dT, \tag{58}$$

$B_2 = C_2,$
$B_1 = C_1 + C_2 T_{in} / 2,$
$B_0 = C_0 + C_1 T_{in} + C_2 T_{in}^2.$

Using Eq. (55), the solution of Eq. (57) is obtained as

$$X_{i+1} = X_i - (\frac{B_2}{3} X_i^3 + \frac{B_1}{2} X_i^2 + B_0 X_i - C) / (B_2 X_i^2 + B_1 X_i + B_0)$$
$$= (\frac{2B_2}{3} X_i^3 + \frac{B_1}{2} X_i^2 + C) / (B_2 X_i^2 + B_1 X_i + B_0). \tag{59}$$

V.B Outside Temperature of Capsule

The outside temperature of the capsule (or cladding) at axial position n is calculated

$$T_{co}(n) = T_{Na}(n) + q(n)/(2\pi r_{co} h_c), \tag{60}$$

where

$q(n) = q_{avg} \times NF \times QSF(n) / \sum_{i=1}^{NF} QSF(i)$: linear power,

$h_c = k_{Na} Nu / D_e = k_{Na} (5 + 0.025(Pe)^{0.8}) / D_e$: heat transfer coefficient,

D_e : equivalent diameter,
k_{Na} : thermal conductivity,
$Nu = 5 + 0.025(Pe)^{0.8}$: Nusselt number,

$Pe = D_e v \rho C_p / k_{Na}$: Peclet number.

V.C Inside Temperature of Capsule

Across the capsule wall the one-dimensional heat conduction equation is integrated

$$\int_{T_{co}}^{T_{ci}} k_c dT = -\frac{q(n)}{2\pi}\int_{r_{co}}^{r_{ci}} \frac{1}{r} dr \tag{61}$$

where

$k_c = A_1 + A_2\, T$: thermal conductivity of capsule.

The temperature at radial position i becomes

$$T_c(n,i) = T_{co} + \frac{(q(n)/\pi)\ln(r_{co}/r(n,i))}{A_1 + A_2 T_{co} + \sqrt{(A_1 + A_2 T_{co})^2 + (A_2 q(n)/\pi)\ln(r_{co}/r(n,i))}} \tag{62}$$

proof)

$$\int_{T_{co}}^{T_{co}+X} (A_1 + A_2 T) dT = -\frac{q(n)}{2\pi}\ln(r_{ci}/r_{co}), \tag{63}$$

$$A_1 X + \frac{A_2}{2} X^2 + A_2 T_{co} X + \frac{q(n)}{2\pi}\ln(r_{ci}/r_{co}) = 0. \tag{64}$$

The root of Eq. (64) is

$$X = \frac{-(A_1 + A_2 T_{co}) + \sqrt{(A_1 + A_2 T_{co})^2 - A_2 q(n)/\pi \times \ln(r_{ci}/r_{co})}}{A_2}$$

$$= \frac{q(n)/\pi \times \ln(r_{co}/r_{ci})}{(A_1 + A_2 T_{co}) + \sqrt{(A_1 + A_2 T_{co})^2 + A_2 q(n)/\pi \times \ln(r_{co}/r_{ci})}} \tag{65}$$

V.D Outside Temperature of Clad

The temperature is determined by iteration (Newton-Raphson method) with the capsule-clad bond (usually sodium) conductivity given as a quadratic function of temperature.

Clad inner surface temperature is also obtained similar as Eq.(65).

The average temperature and average thermal expansion are given as

$$\overline{T_c} = \int_{r_{co}}^{r_{ci}} T \cdot r\, dr \Big/ \int_{r_{co}}^{r_{ci}} r\, dr, \tag{66}$$

$$\overline{\alpha T}_c = \int_{r_{co}}^{r_{ci}} \alpha_c \cdot T \cdot r\, dr \Big/ \int_{r_{co}}^{r_{ci}} r\, dr, \tag{67}$$

where

$\alpha_c = 8.778\times10^{-6} + 1.466\times10^{-10} T$, $^{o}F^{-1}$: thermal expansion coefficient of cladding.

Eqs. (66) and (67) are obtained from numerical integration (7-point Newton-Cote numerical

integration):

$$\int_{x_1}^{x_6} f(x)dx = \frac{h}{140}(41f_1 + 216f_2 + 27f_3 + 272f_4 + 27f_5 + 216f_6 + 41f_7) - \frac{9}{1400}h^9 f^{(8)}(\varepsilon) \tag{68}$$

From a mass balance and values of r_0, r_1, and r_2,

$$\pi R^2\rho_3 = \pi(r_1^2 - r_0^2)\rho_1 + \pi(r_2^2 - r_1^2)\rho_2 + \pi(R^2 - r_2^2)\rho_3, \tag{69}$$

we find the radius of the void to be

$$r_0^2 = r_2^2\frac{\rho_2 - \rho_3}{\rho_1} + r_1^2\frac{\rho_1 - \rho_2}{\rho_1} \tag{70}$$

Heat-generation rate in the regions:

$$H_3 = \frac{P}{\pi R^2}, \quad \text{P: linear power} \tag{71a}$$

$$H_2 = \frac{P}{\pi R^2}\frac{\rho_2}{\rho_3}, \tag{71b}$$

$$H_1 = \frac{P}{\pi R^2}\frac{\rho_1}{\rho_3}. \tag{71c}$$

Heat-conduction equation:

$$\frac{1}{r}\frac{d}{dr}\left(rk_3\frac{dT}{dr}\right) = -H_3 \tag{72}$$

Integration of Eq. (72) once yields

$$k_3\frac{dT}{dr} = -\frac{1}{2}H_3 r + \frac{C_3}{r}. \tag{73}$$

A second integration yields

$$\int_{T_s}^{T_2} k_3 dT = \frac{1}{4}H_3R^2\left[1 - \left(\frac{r_2}{R}\right)^2\right] - C_3\ln\left(\frac{R}{r_2}\right) \tag{74}$$

Similarly, the first and second integrals of the heat-conduction equation in regions 2 and 1 are

$$k_2\frac{dT}{dr} = -\frac{1}{2}H_2 r + \frac{C_2}{r} \tag{75}$$

$$\int_{T_2}^{T_1} k_2 dT = \frac{1}{4}H_2r_2^2\left[1 - \left(\frac{r_1}{r_2}\right)^2\right] - C_2\ln\left(\frac{r_2}{r_1}\right) \tag{76}$$

$$k_1\frac{dT}{dr} = -\frac{1}{2}H_1 r + \frac{C_1}{r} \tag{77}$$

$$\int_{T_1}^{T_0} k_1 dT = \frac{1}{4}H_1r_1^2\left[1 - \left(\frac{r_0}{r_1}\right)^2\right] - C_1\ln\left(\frac{r_1}{r_0}\right) \tag{78}$$

Three boundary conditions to determine constants C_1, C_2, C_3:

$$k_3\left(\frac{dT}{dr}\right)_{r=r_2} = k_2\left(\frac{dT}{dr}\right)_{r=r_2}, \tag{79}$$

$$k_2\left(\frac{dT}{dr}\right)_{r=r_1} = k_1\left(\frac{dT}{dr}\right)_{r=r_1}, \tag{80}$$

$$\left(\frac{dT}{dr}\right)_{r=r_0} = 0. \tag{81}$$

Eqs. (78) and (81) shows that

$$C_1 = \frac{1}{2}H_1 r_0^2 = \frac{1}{2}\left(\frac{P}{\pi R^2}\right)\left(\frac{\rho_1}{\rho_3}\right)r_0^2 \tag{82}$$

Similarly, C_2 is found to be

$$\begin{aligned} C_2 &= \frac{1}{2}H_2 r_1^2 - \frac{1}{2}H_1(r_1^2 - r_0^2) \\ &= \frac{1}{2}\left(\frac{P}{\pi R^2}\right)\left[\left(\frac{\rho_2}{\rho_3}\right)r_1^2 - \left(\frac{\rho_1}{\rho_3}\right)(r_1^2 - r_0^2)\right] \end{aligned} \tag{83}$$

C_3 is

$$\begin{aligned} C_3 &= \frac{1}{2}H_3 r_2^2 - \frac{1}{2}H_2(r_2^2 - r_1^2) - \frac{1}{2}H_1(r_1^2 - r_0^2) \\ &= \frac{1}{2}\left(\frac{P}{\pi R^2}\right)\left[r_2^2 - \left(\frac{\rho_2}{\rho_3}\right)(r_2^2 - r_1^2) - \left(\frac{\rho_1}{\rho_3}\right)(r_1^2 - r_0^2)\right] = 0 \end{aligned} \tag{84}$$

Substitution of these expressions for C_1, C_2, and C_3 into Eqs. (82), (83), and (84) yields the final formulas for the conductivity integrals in the three annular zones:

$$\int_{T_s}^{T_2} k_3 dT = \frac{P}{4\pi}\left[1 - \left(\frac{r_2}{R}\right)^2\right], \tag{85}$$

$$\int_{T_2}^{T_1} k_2 dT = \left(\frac{P}{4\pi}\right)\left(\frac{\rho_2}{\rho_3}\right)\left(\frac{r_2}{R}\right)^2\left[1 - \left(\frac{r_1}{r_2}\right)^2 - \left(1 - \frac{\rho_3}{\rho_2}\right)\ln\left(\frac{r_2}{r_1}\right)^2\right], \tag{86}$$

$$\int_{T_1}^{T_0} k_1 dT = \left(\frac{P}{4\pi}\right)\left(\frac{\rho_1}{\rho_3}\right)\left(\frac{r_1}{R}\right)^2\left[1 - \left(\frac{r_1}{r_2}\right)^2 - \left(\frac{r_0}{r_1}\right)\ln\left(\frac{r_1}{r_0}\right)^2\right]. \tag{87}$$

If $r_0 = 0$ (homogeneous with equal density, $\rho_1 = \rho_2 = \rho_3$), the constants C_1, C_2, and C_3 are

$$C_1 = \frac{1}{2}H_1 r_0^2 = 0, \tag{88a}$$

$$C_2 = \frac{1}{2}H_2 r_1^2 - \frac{1}{2}H_1 r_1^2 = \frac{1}{2}\left(\frac{P}{\pi R^2}\right)\left[\left(\frac{\rho_2}{\rho_3}\right)r_1^2 - \left(\frac{\rho_1}{\rho_3}\right)r_1^2\right] = 0, \tag{88b}$$

$$C_3 = 0. \tag{88c}$$

The final formulas for the conductivity integrals in the three annular zones

$$\int_{T_s}^{T_2} k_3 dT = \frac{P}{4\pi}\left[1 - \left(\frac{r_2}{R}\right)^2\right], \tag{89a}$$

$$\int_{T_2}^{T_1} k_2 dT = \left(\frac{P}{4\pi}\right)\left(\frac{r_2}{R}\right)^2\left[1-\left(\frac{r_1}{r_2}\right)^2\right], \tag{89b}$$

$$\int_{T_1}^{T_0} k_1 dT = \left(\frac{P}{4\pi}\right)\left(\frac{r_1}{R}\right)^2. \tag{89c}$$

VI. SUMMARY AND CONCLUSION

From the review results of four computer code systems, a brief summary of temperature calculation algorithm is provided in Table III. Finite difference method is used to obtain temperature distribution and a one-dimensional approximation is also used. It needs proven thermal models of pellet and cladding. In the case of LIFE, the thermal model used is out of date, thus new thermal models should be considered to obtain the accurate temperature distribution. Recently, the Argonne National Laboratory (ANL) has updated LIFE code and added new options to cover metal fuels.

The ultimate purpose of the fuel-pin analysis is that given the geometry of the fuel element (i.e., the fuel radius, the cladding thickness, and the size of the fuel-cladding gap), the initial chemical composition and porosity of the fuel, and the power history during the irradiation of fuel are predicted by the length of time that the cladding performs its primary function of separating the coolant from the fuel. A fuel element is considered to have failed when the cladding is breached. To predict of the behavior of fuel element, computer analyses which are called fuel-modeling codes attempt to follow the evolution of the important characteristics of the fuel and cladding as functions of irradiation time, beginning with the first application of power and terminating in failure by cladding rupture. The present review simply compared temperature calculation algorithms of several fuel-modeling codes with concentrating on the calculation methods. In a near future, the mechanical computation algorithms will be also investigated. These data will be utilized to construct computing code systems for dry process fuel rod performance.

References

1. D.R. Olander, *Fundamental Aspects of Nuclear Reactor Fuel Elements*, Technical Information Center, U.S. Department Energy. 1976.
2. G.A. Berna, et.al., *FRAPCON-3 A Computer Code for the Calculation of Steady-State, Thermal Mechanical Behavior of Oxide Fuel Rods for High Burnup*, NUREG/CR-6534, PNNL-11513, Pacific Northwest National Laboratory, 1997.
3. M. Suzuki, *Light Water Reactor Fuel Analysis Code FEMAXI-V (Ver.1)*, JAERI-Data/Code 2000-030, Japan Atomic Energy Research Institute, 2000.
4. H.C. Suk, et.al., *ELESTRES.M11K Program Users' Manual and Description*, KAERI/TR-320/92, Korea Atomic Energy Research Institute, 1992
5. V.Z. Jankus and R.W. Weeks, LIFE-I, a FORTRAN-IV Computer Code for the Prediction of Fast-reactor Fuel-element Behavior, ANL-7736, Argonne National Laboratory, 1970

Table I. Characteristics of Fuel Rod Performance Code Systems

Code(Rx type)	Developer	Issue Year	Characteristics
FRAPCON-3 (PWR, BWR)	PNNL INEEL	1980 ~ 1997	Sufficiently slow changes of power and boundary conditions (steady-state)
FEAMXI-V (PWR, BWR)	JAERI	1986 ~ 2000	Normal operation and transient conditions (load-following and rapid power incease) Boling transition of BWR
ELESTRES (CANDU)	AECL	1986	Connected several codes: FEAST, FEAT, BEAM, BOW, etc Pellet and cladding contact condition
LIFE-I (FBR)	ANL	1970	In-pile behavior of cylindrical fast-reactor ceramic fuel elements including mixed oxide fuel (MOX)

PNNL: Pacific Northwest National Laboratory

INEEL: Idaho National Engineering and Environmental Laboratory

JAERI: Japan Atomic Energy Research Institute

AECL: Atomic Energy of Canada Limited

ANL: Argonne National Laboratory

Table II. Phenomena Analyzed by FEMAXI-V

	Thermal process determining temperature distribution	Process with mechanical displacement
Pellet	Thermal conduction (heat flux distribution) FP gas release (depending on Temperature and burnup level)	Thermal expansion, elasticity, Plasticity, creep, cracking, initial relocation, densification, swelling (by solid FP, gas bubble), hot-press
Cladding	Thermal conduction, Waterside corrosion	Thermal expansion, elasticity, Plasticity, creep, irradiation growth
Fuel rod	Gap thermal conduction (mixed gas, contact, radiation), cladding surface heat transfer, gap gas flow	Mechanical interaction between pellet and cladding, friction

Table III. Summary of Thermal Algorithms

	FRAPCON-3	FEMAXI-V	ELESTRES.M11K	LIFE-I
Pellet thermal conductivity	Lucuta's model	Optional	MATPRO-11	Sayles' model (1967)
Cladding thermal conductivity	Anderson's model (1972)	MATPRO-9	MATPRO-11	Bump's model (1970)
Computing dimension	One-dimensional	Two-dimensional (time + space)	One-dimensional	One-dimensional
Computing method	FDM	FDM	FDM + Analytic (Quadratic approximation)	Analytic (Newton-Raphson method)

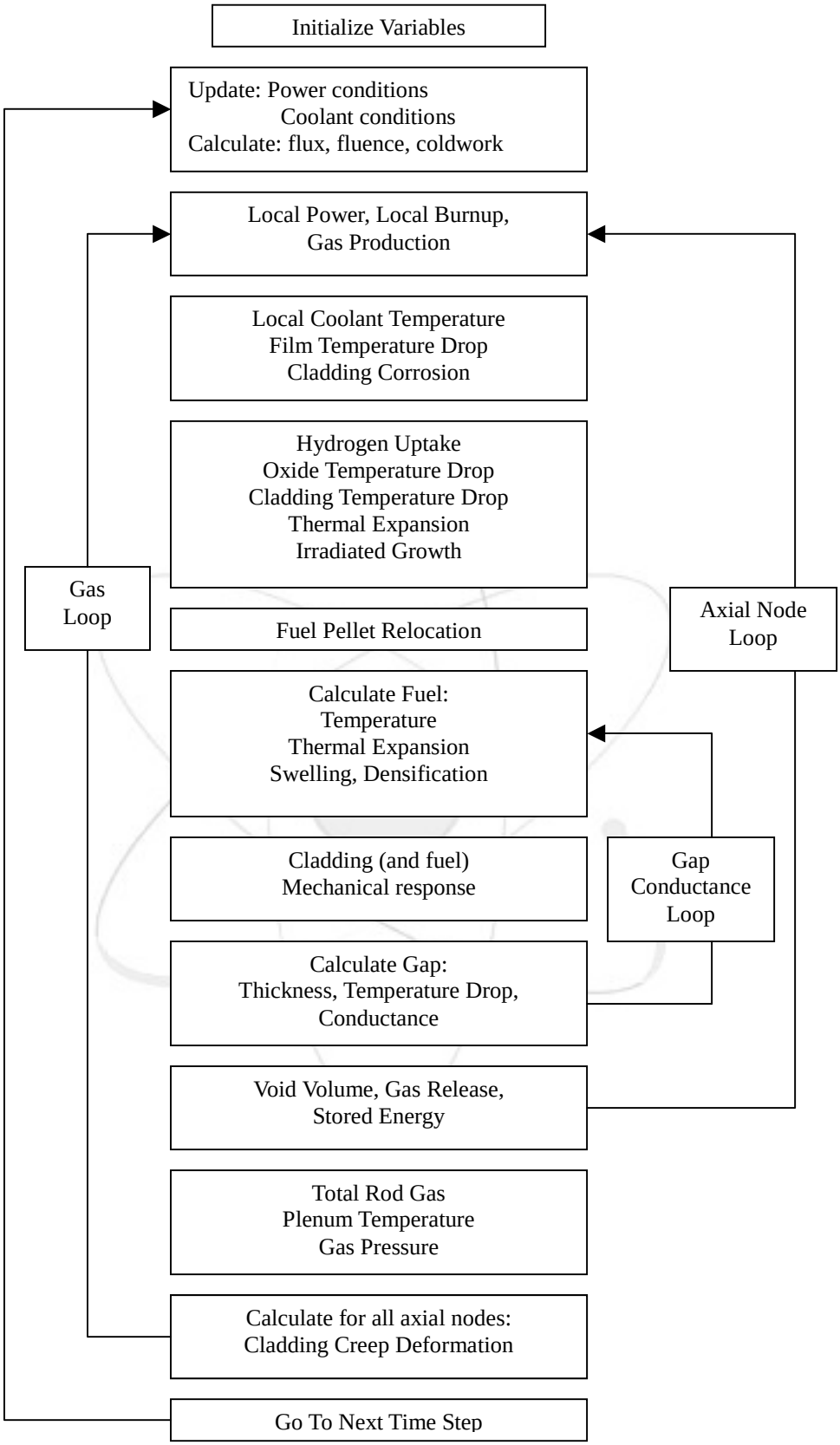

Figure 1. Flowchart of FRAPCON-3.

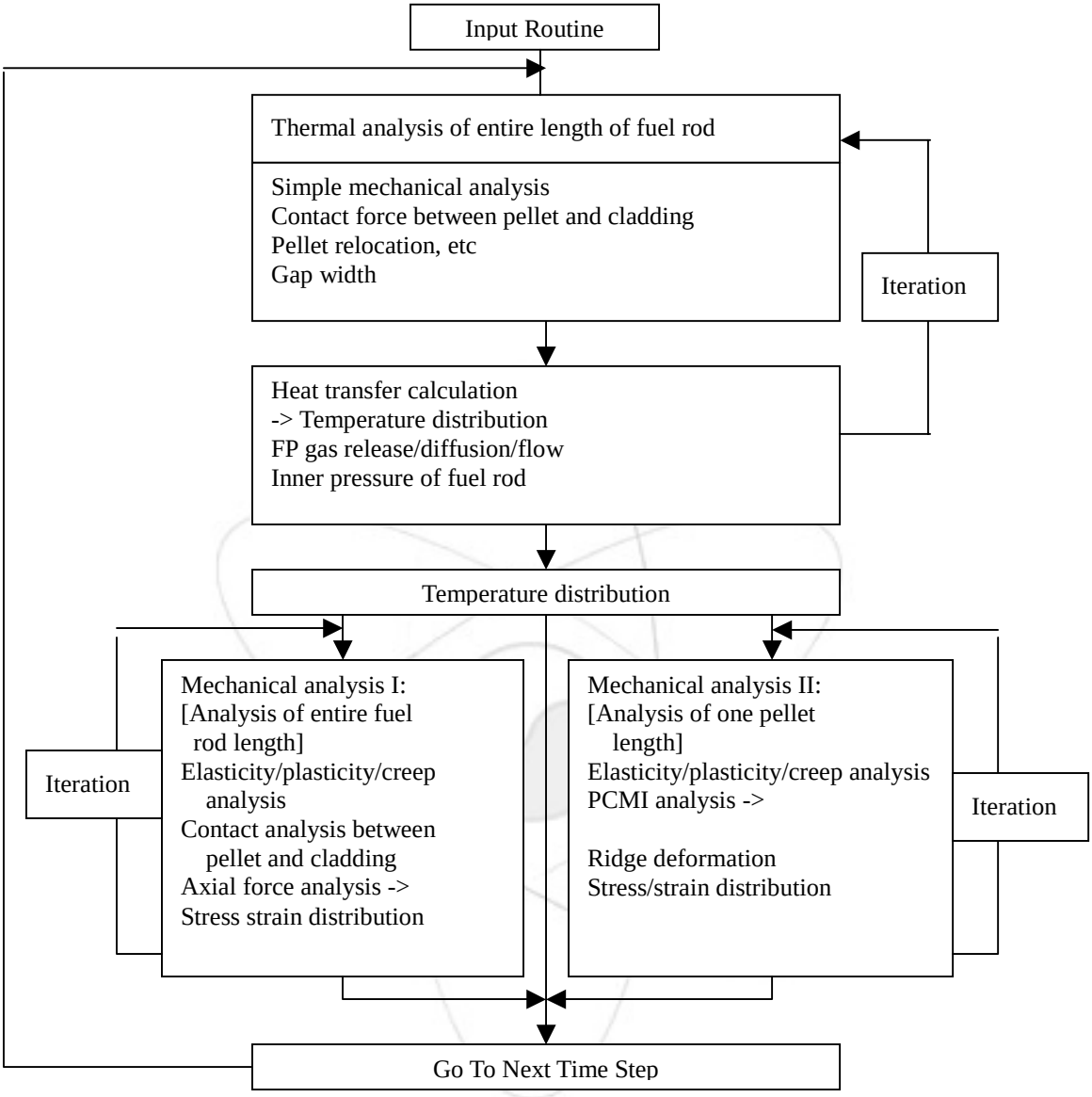

Figure 2. Flowchart of FEMAXI-V.

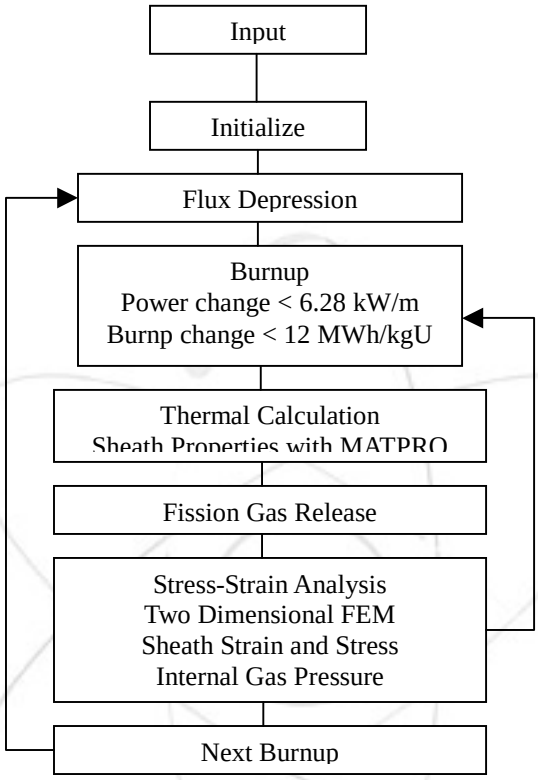

Figure 3. Flowchart of ELESTRES.

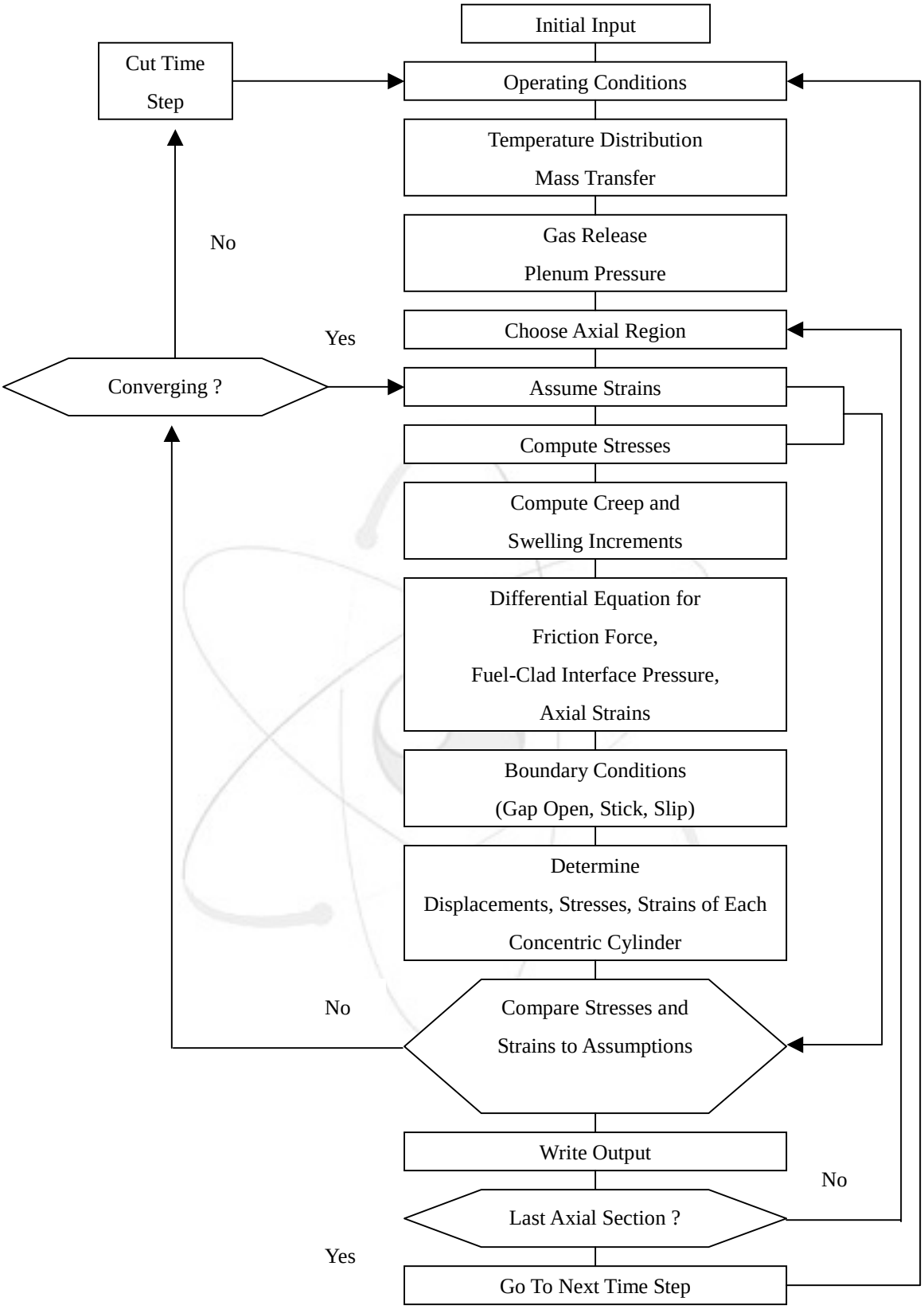

Figure 4. Flowchart of LIFE-1.

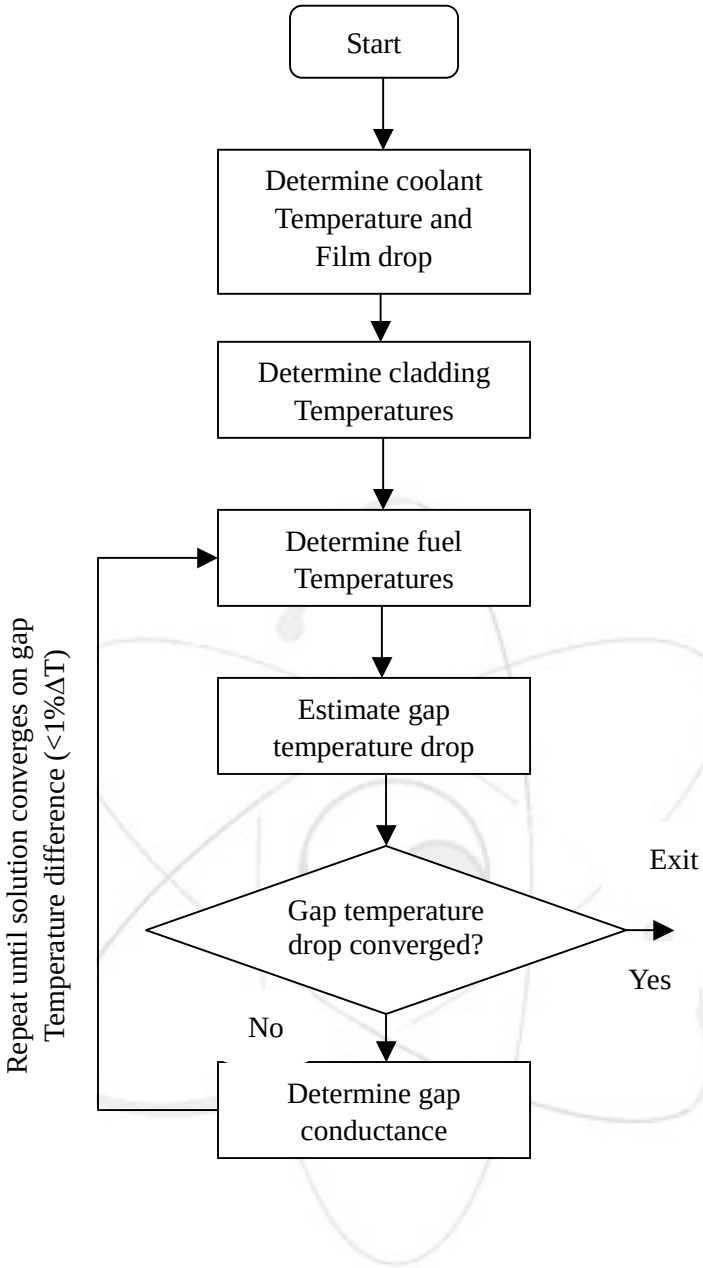

Figure 5. Flow chart of the fuel and cladding temperature calculation.

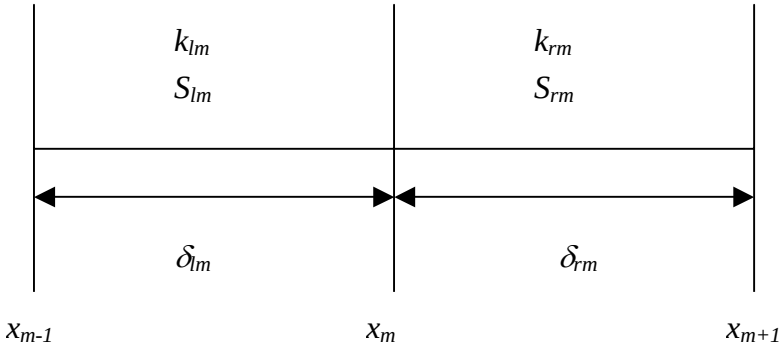

Figure 6. Typical mesh points for pellet thermal model in FRAPCON-3.

BIBLIOGRAPHIC INFORMATION SHEET

Performing Org. Report No.	Sponsoring Org. Report No.	Standard Report No.	INIS Subject Code
KAERI/TR-2586/2003			

Title/Subtitle	A Comparison of Thermal Algorithms of Fuel Performance Code Systems
Main Author	C.J. Park (Dry process fuel technology development)
Researcher and Department	J.H. Park, K.H. Kang, H.J. Ryu, J.S. Moon, I.H. Jeong, C.Y. Lee, K.C. Song (Dry process fuel technology development)

Publication Place	Taejon	Publisher	KAERI	Publication Date	2003. 11.
Page	43 p.	Ill. & Tab.	Yes (V), No ( )	Size	26 Cm.
Note					

Classified	Open ( ), Restricted ( ), Class Document, Internal Use Only (V)	Report Type	Technical Report
Sponsoring Org.		Contract No.	

Abstract (15-20 Lines)

The goal of the fuel rod performance is to identify the robustness of a fuel rod with cladding material. Computer simulation of the fuel rod performance becomes one of important parts to designed and evaluate new nuclear fuels and claddings. To construct a computing code system for the fuel rod performance, several algorithms of the existing fuel rod performance code systems are compared and are summarized as a preliminary work. Among several code systems, FRAPCON, and FEMAXI for LWR, ELESTRES for CANDU reactor, and LIFE for fast reactor are reviewed. Thermal algorithms of the above codes are investigated including methodologies and subroutines. This work will be utilized to construct a computing code system for dry process fuel rod performance.

Subject Keywords (About 10 words)	Fuel performance code, FRAPCON, FEMAXI, ELESTRES, LIFE, thermal algorithm

서 지 정 보 양 식

수행기관보고서번호	위탁기관보고서번호	표준보고서번호	INIS 주제코드
KAERI/TR-2586/2003			

제목/부제	핵연료성능평가코드들의 온도계산 알고리듬 비교

연구책임자 및 부서명	박창제 (건식공정핵연료기술개발부)
연구자 및 부서명	박주환,강권호,류호진,문제선,정인하,이철용,송기찬 (건식공정핵연료기술개발부)

출 판 지	대전	발행기관	한국원자력연구소	발행년	2003. 11.
페 이 지	43 p.	도 표	있음(V), 없음( )	크 기	26 Cm.
참고사항					

비밀여부	공개(V), 대외비( ), __ 급비밀, 소내만 공개 ( )	보고서종류	기술보고서
연구위탁기관		계약 번호	

초록 (15-20줄내외)

핵연료봉의 성능 목표는 피복재와 핵연료봉의 강건성을 규명하는데 있다. 새로운 원자력시스템의 개발 일환으로 핵연료봉의 성능을 컴퓨터로 모사하는 작업의 필요가 늘어나고 있는 실정이다. 핵연료봉 성능평가전산체계를 구축하기위하여 우선 기존에 이용되는 전산체계의 계산순서를 비교해보고 세부사항을 요약하여 보았다. 여러 전산체계중에서 경수로용인 FRAPCON 과 FEMAXI, CANDU 원자로용인 ELESTRES, 그리고 고속로용인 LIFE 등을 선정하여 비교하였다. 각 방법론과 서버루틴을 포함하여 면밀히 온도 계산 순서 알고리듬을 분석하였다. 이러한 작업은 향후 건식재가공 핵연료 성능평가 시스템에 유용한 자료로 활용될 것이다.

주제명키워드 (10단어내외)	핵연료성능평가전산체계, FRAPCON, FEMAXI, ELESTRES, LIFE, 온도계산순서 알고리듬